HHS Public Access

Author manuscript

J Bone Miner Res. Author manuscript; available in PMC 2020 August 12.

Published in final edited form as:

J Bone Miner Res. 2019 December ; 34(12): 2287–2300. doi:10.1002/jbmr.3857.

Hop2 Interacts with ATF4 to Promote Osteoblast Differentiation

Yang Zhang[1,2], **Tonghui Lin**[1], **Na Lian**[1], **Huan Tao**[3], **Cong Li**[1], **Lingzhen Li**[4], **Xiangli Yang**[1]

[1]Pediatric Research Center, Department of Pediatrics, UTHealth McGovern Medical School, Houston, TX, USA

[2]Department of Orthopaedic Surgery, Division of Orthopaedics, Nanfang Hospital, Southern Medical University, Guangzhou, China

[3]Department of Medicine, Division of Cardiovascular Medicine, Vanderbilt University Medical Center, Nashville, TX, USA

[4]Department of Molecular and Human Genetics, Baylor College of Medicine, Houston, TX, USA

Abstract

Activating transcription factor 4 (ATF4) is a member of the basic leucine zipper (bZip) transcription factor family required for the terminal differentiation of osteoblasts. Despite its critical importance as one of the three main osteoblast differentiation transcription factors, regulators of osteoblast terminal maturation remain poorly defined. Here we report the identification of homologous pairing protein 2 (Hop2) as a dimerization partner of ATF4 in osteoblasts via the yeast two-hybrid system. Deletional mapping revealed that the Zip domain of Hop2 is necessary and sufficient to bind ATF4 and to enhance ATF4-dependent transcription. Ectopic Hop2 expression in preosteoblasts increased endogenous ATF4 protein content and accelerated osteoblast differentiation. Mice lacking *Hop2* (*Hop2*$^{-/-}$) have a normal stature but exhibit an osteopenic phenotype similar to the one observed in *Atf4*$^{-/-}$ mice, albeit milder, which is associated with decreased *Osteocalcin* mRNA expression and reduced type I collagen synthesis. Compound heterozygous mice (*Atf4*$^{+/-}$:*Hop2*$^{+/-}$) display identical skeletal defects to those found in *Hop2*$^{-/-}$ mice. These results indicate that Hop2 plays a previous unknown role as a determinant of osteoblast maturation via its regulation of ATF4 transcriptional activity. Our work for the first time reveals a function of Hop2 beyond its role in guiding the alignment of homologous chromosomes.

Keywords

ATF4; HOP2; TRANSCRIPTION FACTOR; OSTEOBLAST; DIFFERENTIATION

Address correspondence to: Xiangli Yang, PhD, Department of Pediatrics, Pediatric Research Center, UTHealth McGovern Medical School, 6431 Fannin Street, MSE R428, Houston, TX 77030, USA. xiangli.y.elefteriou@uth.tmc.edu.

Authors' roles: Study design: XY. Study conduct and data collection: YZ, TL, NL, LL, CL, and HT. Data analysis and manuscript drafting: XY, YZ, and NL.

Disclosures

All authors state that they have no conflicts of interest.

Additional Supporting Information may be found in the online version of this article.

Introduction

Osteoblasts are bone-forming cells that originate from multipotent mesenchymal stem cells (MSCs). The proliferation and differentiation of MSCs are ultimately controlled by lineage-specific transcription factors (TFs). Three osteoblast-specific transcription factors were identified thus far, namely Runx2 (Runt-related TF 2), Osterix (Osx or SP7), and activating transcription factor 4 (ATF4). Runx2 and Osx are considered as master regulators of the osteoblast lineage because they are expressed very early in this lineage and act sequentially to specify this cell type. Mice lacking either *Runx2* or *Osx* have a skeleton that consists of cartilage only and die of respiratory failure soon after birth.[1,2]

Unlike Runx2 and Osx, the mRNA of *Atf4* is ubiquitously expressed during embryonic development and throughout life, but the protein of ATF4 is restricted to committed osteoblasts.[3]

ATF4 was first identified as an osteoblastic-specific nuclear activity that binds to the osteoblastic-specific element 1 (OSE1) of *Ocn*.[2,4] It belongs to the large ATF/CREB basic leucine zipper (bZip) family of transcription factors that bind to the cAMP response element (CRE), *TGACGTCA*, an octanucleotide motif that is present in the promoter region of a wide variety of genes.[5] These bZip proteins share significant sequence similarity within their Zip domain and an adjacent basic motif. The basic region is responsible for DNA sequence recognition and binding, whereas the Zip domain is a well-studied common structural motif that mediates dimerization between the members of the Zip family to form homo- or heterodimers to regulate gene transcription.[6,7]

ATF4 regulates several aspects of osteoblast biology ranging from the onset of differentiation, endoplasmic reticulum stress response, and cell survival to cell-specific gene expression. We have previously found that although not interacting directly, ATF4 and Runx2 synergistically activate the osteoblastic-specific gene *Osteocalcin* (*Ocn*) in committed osteoblasts.[8] Moreover, ATF4 regulates type I collagen synthesis through a posttranscriptional mechanism. Failure of ATF4 phosphorylation by RSK2 contributes to the skeletal manifestations of patients with Coffin-Lowry Syndrome, an X-linked dominant genetic disorder associated with mental and developmental retardations.[9] The majority of the mice lacking ATF4 die prematurely and display a spectrum of abnormalities including severely decreased bone and fat mass, infertility, blindness, and increased glucose tolerance.[9–13] ATF/CREB bZip transcription factors are known to be ubiquitously expressed, thus the specific nuclear binding activity of ATF4 in osteoblasts raised the hypothesis that ATF4 may dimerize with other proteins that stabilize it in osteoblasts. This hypothesis was supported by our previous observations that ATF4 in non-osteoblastic cells is constantly made and degraded through a ubiquitin-mediated protein degradation mechanism.[3] Another mechanism to explain that ATF4 is a short-lived protein in non-osteoblastic cells could be due to a selective translation in those cells under stress conditions.[14,15]

Based on the presence of leucine zippers in ATF4 and the restricted distribution of its protein in the osteoblast lineage, we hypothesized that ATF4 interacts with other Zip-containing proteins in MSCs to tune the expression and function of target genes in osteoblasts. To

search for such partners of ATF4, we used purified ATF4 as a bait and pulled out vimentin, an intermediate filament (IF) protein, as a partner of ATF4 from the nuclear extracts of ROS 17.2.8 osteosarcoma cells.[16] Our subsequent studies found that vimentin, in response to TGFβ in preosteoblasts, suppresses ATF4-mediated transcription and osteoblast differentiation.[17] In the current study, we have conducted another unbiased search for novel ATF4-interacting proteins via a yeast two-hybrid system and identified homologous pairing protein (Hop2) as a novel partner of ATF4. Our molecular, biochemical, cellular, and genetic evidence demonstrate that Hop2 acts as a coactivator of an osteoblast-specific transcription factor ATF4 to promote osteoblast differentiation.

Materials and Methods

Animals and cell culture

All animal experiments were performed in accordance with the Animals Scientific Procedures Act 1986 and were approved by the local Ethical Review Committee of UTHealth. Experiments were designed in agreement with the ARRIVE guidelines,[18] for the reporting and execution of animal experiments, including sample randomization and blinding. Generation of *Atf4*$^{-/-}$ mice has been described.[12] *Hop2*$^{-/-}$ mice were generously provided by Dr Petukhova (NIH). All mice were housed in individually HEPA-filtered cages with sterile bedding, nesting, and free access to sterilized food and water. Strict littermates of mice were used in this study.

All the cell lines were purchased from ATDC and cultured at 37°C, 5% CO_2. Culture mediums were from Hyclone (Pittsburgh, PA, USA) with supplementation of 10% (v/v) FBS (Atlanta Biologicals, Flowery Branch, GA, USA), and 1% penicillin–streptomycin (Gibco, Thermo Fisher Scientific, Waltham, MA, USA). MC3T3-E1 and permanently overexpressing Hop2 were cultured with αMEM with or without G418 (0.4 mg/mL) and COS1 monkey kidney cells were in DMEM.

Plasmids

Mouse Hop2 cDNA was amplified by RT-PCR using bone cDNA as template and cloned in pcDNA3.1+ mammalian expression vector (Invitrogen, Carlsbad, CA, USA) or pGEX-4T1 bacterial expression vector (Pharmacia Biotech, Piscataway, NJ, USA). Three different truncation forms of mouse Hop2 cDNA, named Hop2$^{1-87}$ (containing amino acids 1–87), Hop2$^{81-147}$ (containing amino acids 81–147), and Hop2$^{141-217}$ (containing amino acids 141–217), respectively, were PCR-amplified and labeled with nuclear location signal (NLS), flanked with cloning sites HindIII and XbaI, and inserted into mammalian expression vector pCMV-HA (Clontech, Mountain View, CA, USA) and bacterial expression vector pGEX-4T1. Mouse ATF4 cDNA was subcloned into pCMV3×Flag (Sigma, St. Louis, MO, USA) from a mammalian expression vector pCMV5-ATF4.[9] The integrity of all cDNA and production of the fusion protein were confirmed by DNA sequencing and Western blot analysis, respectively.

Yeast two-hybrid screening

MATCHMAKER two-hybrid system 3 (Clontech) was used for screening of ATF4-interacting proteins. Full-length as well as different truncated forms of mouse ATF4 cDNA ($ATF4^{36-349}$, $ATF4^{111-349}$, or $ATF4^{251-349}$) were inserted in-frame into pGBT9 GAL4 DNA-BD vector as baits. Yeast strain AH109 (MATa, trp1–901, leu2–3, 112, ura3–52, his3–200, gal4ρ, gal80ρ, LYS2: GAL1UAS-GAL1TATA-HIS3, GAL2UAS-GAL2TATA-ADE2, URA3:: MEL1 UAS-MEL1TATA-LacZ, MEL1) was first transformed with various baits to test for self-activation of different forms of ATF4. AH109 without auto-activation (containing $ATF4^{251-349}$) was subsequently transformed with Clontech mouse testis MATCHMAKER cDNA library and screened on SD/$^{-}$Trp/$^{-}$Leu/$^{-}$Ade/-His with X-α-Gal plates. DNA isolated from positive clones was sequenced using GAL4 DNA-BD Sequencing Primer, and the sequences were blasted with GenBank to analyze the function of the genes (http://www.ncbi.nlm.nih.gov.blast).

Protein chemistry

Bacterially expressed His-tagged and GST-tagged proteins were purified according to the method developed by Novagen (Burlington, MA, USA) as previously described.[19] Nuclear extract (NE) preparation and co-immunoprecipitation (Co-IP) were performed essentially according to the methods described.[4] COS1 cells (85% confluent) in 10-cm plates were transfected with or without 5 μg of Hop2-V5, or together with 5 μg of Flag-ATF4 using lipofectamine (Invitrogen). Cells were treated with 25 μM MG115[3] to stabilize ATF4 for 5 hours before harvesting. Isolated whole-cell lysates were immunoprecipitated with 5 μL of anti-Flag M2 beads (Sigma) for 8 hours at 4°C. After washing three times with ice-cold Tris-buffered saline (50 mM Tris, 150 mM NaCl, pH 7.4), immunocomplexes and NEs as input controls were resolved by SDS-PAGE, transferred onto nitrocellulose membranes, and revealed by Western blotting using anti-Flag M2 or anti-V5 (Invitrogen, Rockford, IL, USA) antibodies. For mapping domains of Hop2 responsible for its interaction with ATF4, pulldown assays were performed with 1 μg of purified GST-Hop2 fusion protein, its variants, or GST (negative control) was incubated with glutathione-Sepharose beads in phosphate-buffered saline buffer (PBS, pH 7.4) at 4°C with rotation for 1 hour and washed three times with PBS buffer, pH 7.4. The beads were then incubated with His-ATF4 at 4°C for 2 hours followed by three washes with PBS, pH 7.4. Bound proteins were eluted by boiling for 5 minutes in 2× SDS sample buffer, separated by SDS-PAGE, and stained with Coomassie Brilliant Blue. To map domains of Hop2, 1 μg of purified His-ATF4 or truncated variants was incubated with Ni-NTA-agarose (Qiagen, Valencia, CA, USA) in PBS, pH 8.0, containing 10 mM imidazole at 4°C with rotation for 1 hour and then washed 3 times with PBS containing 15 mM imidazole. GST-Hop2 was then added and incubated with rotation for 2 hours at 4°C after washing three times with PBS containing 50 mM imidazole. Co-localization of Hop2 and ATF4 were performed by immunohistochemistry in weight sections of embryos of 17.5 days post coitum (E17) and bone tissues of 10-day-old pups (P10). Samples were fixed with 4% PFA for 24 hours at 4°C and decalcified by 10% EDTA (when necessary), tissues were then embedded into paraffin. Sections (5 μm) were processed by immunostaining. The primary antibodies used were anti-Hop2 (Santa Cruz Biotechnology, Dallas, TX, USA, catalog no. sc-514014), anti-ATF4 (Cell Signaling, Danvers, MA, USA, catalog no. 11815). The secondary antibodies used were goat anti-

mouse IgG Alexa Fluor@594 (Abcam, Cambridge, MA, USA, catalog no. ab150116) and goat anti-rabbit IgG Alexa Fluor@647 (Abcam, catalog no. ab150079). DAPI (catalog no. 10236276001) and toluidine blue O (catalog no. T3260) were from Sigma-Aldrich. Fluorescence images were acquired using a laser scanning confocal microscope (LSM800, Carl Zeiss, Thornwood, NY, USA).

DNA binding and transcription assay

DNA transfection and luciferase assays were performed in COS1 cells. Cultured cells were seeded at a density of 5×10^4/well in 24-well plates and transfected with 0.2 μg of the reporter plasmid (p6×*OSE1-Luc*,p*OG2-Luc*, p3×*AP1-Luc*), 0.05 μg of β-galactosidase, 0.2 μg of transcription factor plasmid (pCMV5-ATF4, FosB) with or without 0.2 μg of pcDNA3.1-Hop2 using lipofectamine (Invitrogen). Cells were lysed 24 hours later, and the luciferase activity was normalized to the β-galactosidase activity. Each experiment was performed in triplicate and repeated at least three times. For DNA binding analysis, electrophoretic mobility shift assays (EMSA) were performed with purified His-ATF4 that was incubated with increasing amounts of GST-Hop2 or GST and 5 pmol of a radiolabeled double-stranded OSE1 oligonucleotide[2] at room temperature for 10 minutes as described.[4] For Northern blot analysis, total RNA from different adult mouse tissues or cells was isolated using TRIzol (Invitrogen) according to the manufacturer's protocols. Total RNA (5 μg) was resolved in 1% agarose gel and transferred onto nylon membranes. The membrane was cross-linked by UV light and hybridized following standard protocols with Hop2 cDNA probes with *Gapdh* as loading control. For qRT-PCR, cDNA was prepared using 0.5 μg total RNA, which were then diluted 10-fold for real-time PCR using SYBR green system (Invitrogen). Triplicates for each sample were performed in 3 independent experiments. mRNA levels in each sample were calculated subsequent for the mean Ct. Data were normalized relative to the expression of β-actin. Levels of mRNA were calculated according to appropriate controls under specific experiments and expressed as fold induction using the $2^{-\Delta\Delta Ct}$ method. The primers used for qRT-PCR are shown in Supplemental Table S1.

Differentiation assays

Confluent MC3T3-E1 cells in 12-well plates overexpressing vector (control) or Hop2 were grown in G418-containing medium supplemented with 5 mm β-glycerophosphate and 100 μg/mL ascorbic acid for 7 or 14 days. Crystal violet staining was performed to confirm the equal number of cells seeded on day 0. Mineralization of osteoblasts was assayed by Alizarin red S staining as described.[20] Colony-forming unit (CFU) assays by alkaline phosphatase (ap) staining for primary BMSCs were performed as previously described.[21] Type I collagen synthesis of WT, *Hop2*$^{+/-}$, *Hop2*$^{-/-}$, *Atf4*$^{+/-}$;*Hop2*$^{+/-}$ osteoblasts were performed as previously described. Briefly, cells were labeled with 50 μCi/mL of [^{35}S] methionine and cysteine mix (PerkinElmer, Waltham, MA, USA) for 12 hours in DMEM (methionine and cysteine free; Invitrogen) supplemented with 2% dialyzed FBS, 2 mM L-glutamine, and 55 μM β-mercaptoethanol. The amount of type I collagen was determined as described.[9]

Co-localization

The 17.5-day embryos and bone tissues from 10 days were fixed with 4% PFA for 24 hours at 4°C. After decalcification by 10% EDTA, tissues were embedded into paraffin wax. Five-μm-thick sections were prepared and processed by immunostaining. The primary antibodies used were anti-Hop2 (Santa Cruz, catalog no. sc-514014) and anti-ATF4 (Cell Signaling, catalog no. 11815). The secondary antibodies used were Goat anti-Ms IgG Alexa Fluor@594 (Abcam, catalog no. ab150116) and Goat anti-Rb IgG Alexa Fluor@647 (Abcam, Cat#ab150079). DAPI (catalog no. 10236276001) and Toluidine blue O (catalog no. T3260) were from Sigma-Aldrich. Fluorescence images were acquired using a laser scanning confocal microscope (LSM800, Carl Zeiss).

Bone phenotyping

Micro-computed tomography (micro-CT) analysis was performed as described.[17] Briefly, the skeletons were harvested from mice of various ages and genotypes and fixed overnight in 10% formalin and then 70% ethanol. Femurs and lumbar vertebrae were dissected and placed into a 16-mm sample holder filled with 70% ethanol and scanned by a Scanco μCT-40 desktop micro-CT scanner (Scanco Medical, Bruttisellen, Switzerland) for quantification of bone parameters. The femoral and vertebral bone parameters were obtained, using the Scanco Analysis Software, from the femoral distal metaphyseal section and the vertebral body L_4. The operators were blinded to conduct the analyses. The parameters obtained and analyzed included bone volume to total volume ratio (BV/TV), trabecular number (Tb.N), trabecular thickness (Tb.Th), and trabecular separation (Tb.Sp). For bone histology and histomorphometry, lumbar vertebrae were dissected and fixed for 24 hours in 10% buffered formalin, dehydrated in a graded ethanol series, and embedded in methylmethacrylate resin, sectioned at 5 or 7 μm, and stained by von Kossa/van Gieson. Lumbar spines (7 μm) were then analyzed using the BioQuant Osteo Image Analysis System (Nashville, TN, USA). The parameters comply with the guidelines of the American Society of Bone and Mineral Research nomenclature committee.[22] For analysis of osteoblasts and osteoclasts, 5-μm sections were stained with toluidine blue and tartrate-resistant acid phosphatase (TRAP), respectively. For dynamic histomorphometry, calcein was dissolved in buffer (0.15 M NaCl, 2% $NaHCO^3$) and injected twice intraperitoneally (20 μg/g of body weight) at 7 and 2 days before euthanasia.

Statistical analysis

Statistical analyses on groups of two were performed using one-way ANOVA or paired *t* test for the littermates comparison. A p value <0.05 was considered to be statistically significant.

Results

Identification of Hop2 as an ATF4-interacting protein

Mouse and human ATF4 share 90% homology in their protein sequence. The ATF4 consists of 349 amino acids, which is shorter than its human ortholog by two amino acid residues. Because ATF4 is a transcription activator with two Zip motifs, we constructed a bait plasmid with a partial ATF4 cDNA sequence by removing 241 amino acids from the N-terminus of

the protein to eliminate the intrinsic transcription activation that would otherwise give rise to false-positive signals.[8] This resulting plasmid contains a partial cDNA encoding only the last 98 amino acids that covers the basic and Zip2 domains of mouse ATF4, which was then used as a bait to screen a mouse cDNA library (Clontech). Among the putative interactors, Hop2, a homologous pairing protein, caught our attention because it contains a Zip domain, making it a strong candidate for an ATF4 binding partner (Fig. 1A, B).

To confirm the interaction between Hop2 and ATF4 in cells, we performed co-immunoprecipitation assays by ectopically overexpressing Flag-tagged ATF4 and V5-tagged Hop2 in COS1 cells. Western blot showed that anti-Flag antibody precipitated V5-Hop2, and conversely, anti-V5 precipitated Flag-ATF4 protein. No precipitates were detected by IgG or from nontransfected cell lysates (Fig. 1C). To verify a physical interaction and to define the binding domains mediating the dimerization between ATF4 and Hop2, we performed pulldown assays using purified fusion proteins of GST-Hop2 and His-ATF4 from bacteria transformed with these expressing plasmids. Purified GST-Hop2 and its Zip containing truncated variant, GST-Hop2$^{81-147}$, but not the GST alone, pulled down His-tagged full-length ATF4 (Fig. 1D). Reciprocally, purified His-ATF4 full-length and its Zip-containing truncated variants, His-ATF4$^{1-151}$ and His-ATF4$^{186-349}$, pulled down GST-tagged Hop2. The deletional variant lacking the Zip domains, His-ATF4$^{131-221}$, or Ni-charged beads alone, failed to pull down GST-Hop protein (Fig. 1E). There was no apparent self-dimerization observed in our assay conditions. These data indicate that ATF4 and Hop2 interact in cell and in vitro and their binding to each other is mediated by their respective Zip domains.

Hop2 is expressed in osteoblasts

Although Hop2 was originally identified as a key cofactor for meiosis-specific recombination,[23] emerging evidence has revealed that this evolutionarily conserved protein is also expressed in some somatic tissues, primary human fibroblasts, and various cancer cells, where it was shown to facilitate DNA recombination to repair damaged DNA.[24,25] To determine whether the in vivo function of Hop2 lies beyond the reproductive organs, we analyzed the expression pattern of *Hop2*. Northern blot hybridization revealed that its mRNA is highly expressed in testis, fat, and eye, among other organs (Fig. 2A), which is consistent with previous report,[26] and relevantly, overlaps with organs whose biology is regulated by ATF4.[9,13] Western blot analysis also confirmed that Hop2 is exclusively expressed in the nucleus of MC3T3-E1 preosteoblasts, calvarial cells, and bone marrow stromal cells (BMSCs) (Fig. 2B), all of which serve as precursors of osteoblasts and can be induced to differentiate into mature osteoblasts upon osteogenic induction in vitro.[16,27] Interestingly, the Hop2 protein is expressed at higher level in preosteoblasts compared with fully differentiated osteoblasts, which is consistent with the protein expression pattern of ATF4 (Fig. 2C,D). Finally, Hop2 and ATF4 are co-localized in primary calvarial osteoblasts (Fig. 2E). Thus, the expression pattern of Hop2 at both mRNA and protein levels make it a likely physiological partner of ATF4.

Hop2$^{-/-}$ mice are osteopenic

To determine whether Hop2 regulates osteoblast differentiation and function in a similar manner to ATF4 in vivo, we analyzed *Hop2* mutant mice,[23] with particular attention given to those defects observed in *Atf4*$^{-/-}$ mice.[9–11,28] *Hop2* heterozygous (*Hop2*$^{+/-}$) mice are fertile and able to reproduce at a normal Mendelian ratio (Table 1) with no gross changes in any of the somatic tissues examined. In agreement with the original report describing these mutant mice,[23] *Hop2* homozygous (*Hop2*$^{-/-}$) animals are infertile because of lack of mature gametes in both sexes. Characterization of embryos from embryonic day 13 (E13) to postnatal pups by skeletal preparation and staining revealed no discernible difference in the size and staining area of cartilaginous and bony elements (data not shown), indicating that Hop2 does not affect skeletal development.

Analysis of adult animals from 1 to 6 months revealed that the *Hop2*$^{-/-}$ mutants display normal gross size, weight, and blood glucose level compared with their WT littermates (Supplemental Fig. S1A–C). Micro-computed tomography and histological analyses of the long bones of WT, *Hop2*$^{+/-}$, and *Hop2*$^{-/-}$ littermates at 1, 2, and 3 months of age revealed a normal ratio of bone volume per total tissue volume (BV/TV) in mutant mice of both sexes (data not shown). At 4 months of age, however, BV/TV of *Hop2*$^{-/-}$ mice showed a small but consistent reduction that became statistically significant at 6 months of age, at which a 10% reduction in femurs and a 25% reduction in vertebrae were observed compared with WT and their *Hop2*$^{+/-}$ littermates (Fig. 3A–D). Histomorphometrical analysis of additional bone parameters revealed a 20% reduction in trabecular number (Tb.N), which was accompanied by a 25% increased trabecular separation in *Hop2*$^{-/-}$ bones (Tb.Sp) compared with WT controls (Fig. 3E, F). These data suggested that *Hop2* deficiency causes a defect in osteoblast differentiation and/or function. Supporting this notion, calcein labeling followed by histology revealed a 15% decrease in mineralizing surface per bone surface (MS/BS), and a 10% decrease in mineral apposition rate (MAR) (Fig. 3G–I) in 6-month-old mice. Additionally, there was a 20% decrease in the number of osteoblasts per BS (Fig. 3J, K). As expected, osteoclast number per bone surface remained unchanged (Supplemental Fig. S2A). These results demonstrate that Hop2 is required for bone formation in vivo and suggest it regulates osteoblast differentiation or function.

Hop2 regulates osteoblast differentiation and function cell-autonomously

To further define whether the bone phenotype of *Hop2*$^{-/-}$ mice stemmed from a cell-autonomous mechanism, we isolated primary bone marrow stromal cells (BMSCs) from WT and *Hop2*$^{-/-}$ long bones for osteoblast differentiation assays. BMSC cultures were then analyzed on day 0 and on days 7 and 14 after culture in osteogenic conditions as described previously.[21] Compared with WT controls, *Hop2*$^{-/-}$ BMSC cultures had close to 40% fewer alkaline phosphatase positive (ap+) colony-forming units (CFU-ap+) and 30% fewer von Kossa-positive CFUs (CFU-ob+, Fig. 4A) than WT BMSCs. Moreover, qRT-PCR analyses from those cultures at different stages of osteoblast differentiation revealed a reduction in the expression of several osteoblast marker genes, including early-stage marker genes (*Runx2*, *ALP*, and *Col1*) and the late-stage marker gene *Ocn*, an ATF4 direct transcriptional target (Fig. 4B). These results show that *Hop2*$^{-/-}$ BMSCs have an intrinsic

osteogenic defect and are unable to be induced to differentiate as efficiently as their WT controls.

A hallmark of defective function of ATF4 in osteoblasts is that the endogenous expression of *Ocn* by bone and type I collagen synthesis by *Atf4*$^{-/-}$ primary calvarial osteoblasts are decreased.[9] *Ocn* is a marker gene for mature osteoblasts, whereas type I collagen is the most abundant constituent of bone matrix proteins that provide a scaffold for mineralization. Thus, a defective *Ocn* expression and type I collagen synthesis is attributed to the osteopenic phenotype in *Atf4*$^{-/-}$ mice. To understand whether Hop2 is also required for the full activation of endogenous *Ocn*, we performed Northern hybridization and found a 50% decrease in *Ocn* mRNA in *Hop2*$^{-/-}$ long bones compared with WT controls (Fig. 4C). Similarly, a [^{35}S]-methionine incorporation assay showed a 25% reduction in α1 and α2 chains of type I collagen isolated from *Hop2*$^{-/-}$ primary calvarial cells compared with the WT or *Hop2*+/− controls (Fig. 4D). Taken together, these data support that Hop2, similar to ATF4, autonomously regulates *Ocn* expression and type I collagen synthesis in osteoblasts.

Genetic interaction between *Hop2* and *Atf4*

The skeletal abnormalities found in *Hop2*$^{-/-}$ mice are similar, albeit milder, to what were observed in *Atf4*$^{-/-}$ mice, which is not sufficient to establish the genetic interaction between *Hop2* and *Atf4*. We thus sought to determine whether ATF4 and Hop2 would interact under physiological condition. We reasoned that if Hop2 was a physiological partner of ATF4, not only *Hop2*$^{-/-}$ mice but also *Atf4*:*Hop2* compound heterozygous mice (lacking one copy of each *Atf4* and *Hop2* alleles) would display phenotypic and cellular abnormalities overlapping those in *Hop2*$^{-/-}$ and *Atf4*$^{-/-}$ mice. To test this hypothesis, crosses between *Atf4*$^{+/-}$ and *Hop2*$^{+/-}$ mice were set up and mice of WT, single, and double heterozygous animals were obtained. Skeletal parameter analyses showed that single heterozygous of *Atf4*$^{+/-}$ or *Hop2*$^{+/-}$ were indistinguishable from WT littermates. However, *Atf4*$^{+/-}$:*Hop2*$^{+/-}$ mice displayed a decreased BV/TV, trabecular number, and thickness in both long bones and vertebrae compared with *Hop2*$^{+/-}$ or *Atf4*$^{+/-}$ controls (Fig. 5A–E). The defects are also rooting from a defective function of osteoblasts as shown by decreased mineralization surface per bone surface, mineral apposition rate, and osteoblast count in *Atf4*$^{+/-}$:*Hop2*$^{+/-}$ bones compared with single heterozygous controls (Fig. 5F–J and Supplemental Fig. S2B). Not surprisingly, cultured BMSCs from *Atf4*$^{+/-}$:*Hop2*$^{+/-}$ long bones formed fewer CFU-ap + and CFU-ob + colonies than that of controls (Fig. 6A, B), which was consistent with qRT-PCR analysis of the expression levels of osteoblast marker genes (Fig. 6C). Finally, primary calvarial cells from *Atf4*$^{+/-}$:*Hop2*$^{+/-}$ had a 25% reduction in [^{35}S]-methionine incorporation into α1 and α2 chains of type I collagen compared with single heterozygous osteoblasts (Fig. 6D). Collectively, these lines of genetic, phenotypic, and molecular evidence establish that Hop2 is the physiological partner of ATF4 in osteoblasts.

Hop2 enhances ATF4-mediated transcription

A physical interaction between Hop2 and ATF4 together with the similar bone defects found in both *Hop2*$^{-/-}$ (Fig. 3) and *Atf4*$^{-/-}$[9] mice strongly suggested Hop2 might act as a physiological partner of ATF4 in vivo. Because Hop2 lacks the basic region common in the bZip transcription factors (Fig. 1B), we hypothesized that Hop2 affects gene transcription

via its binding to ATF4. To test this possibility, we cotransfected COS1 cells with Hop2 and ATF4 expression plasmids and with two reporter plasmids, p6x*OSE1-Luc* or p*OG2-Luc*. The p6x*OSE1-Luc* reporter contains a luciferase gene driven by 6 copies of the ATF4 binding site, OSE1, identified in the promoter region of the mouse *Ocn* 2 gene (*OG2*), whereas the p*OG2-Luc* reporter construct contains a 160-bp promoter fragment of the *OG2*.[2,4] Ectopic expression of ATF4 alone activated the p6x*OSE1*-Luc and the p*OG2-Luc* more than 40- and 5-fold, respectively (Fig. 7A, B), which is expected and consistent with our previous findings.[3,16,29] However, ectopic expression of Hop2 alone failed to activate either *OSE1*- or *OG2*-driven reporter (Fig. 7A, B), suggesting that Hop2 itself does not bind to the *OSE1* or to the short native *Ocn* promoter. Interestingly, ectopic expression of both Hop2 and ATF4 augmented the reporter activities driven by 6x*OSE1* more than 60-fold (Fig. 7A) and such superactivation of ATF4 reporter by Hop2 was also observed in ATF4-mediated *pOG2-Luc* reporter (Fig. 7B). This superactivation of Hop2 is specific to ATF4 because Hop2 expression failed to enhance other bZip protein-dependent transcription (Fig. 7C). Supporting this and consistent with our mapping data (Fig. 1D, E), the truncated Zip-containing Hop2$^{81-147}$ variant, but not the Hop2$^{1-87}$ and Hop2$^{141-217}$ variants, was sufficient to convey the superactivation activity as potent as the full-length Hop2$^{1-217}$ (Fig. 7D). These data thus validate the functional relevance of the interaction between Zip motifs of Hop2 and ATF4 in cells.

Ectopic expression of Hop2 accelerates osteoblast differentiation

The loss-of-function studies by analyzing the *Hop2*$^{-/-}$ mice revealed that Hop2 is required for osteoblast differentiation and function in vivo. To understand whether gain of function in Hop2 could stimulate osteoblast differentiation, we established MC3T3-E1 cell lines overexpressing *Hop2* stably. Osteogenic induction of confluent Hop2 permanent and control cells over a time course of 14 days was performed and calcified colonies were visualized by alizarin red (AR) staining. AR-positive colonies were defined as differentiated osteoblasts (ob+) and the number of ob+ colonies were quantified. The number of total ob+ cells on days 7 and 14 after osteogenic induction was doubled in the MC3T3-E1 cells overexpressing *Hop2* compared with control cells (Fig. 7E). This result argues that increased Hop2 expression stimulates osteoblast differentiation in vitro.

Hop2 stabilizes ATF4 in preosteoblasts

To address how Hop2 enhances the transcription activity of ATF4 and stimulates osteoblast differentiation, we tested two possibilities. First, the Hop2-ATF4 heterodimer might bind to OSE1 DNA with higher affinity than ATF4 homodimer; second, Hop2-ATF4 dimerization might stabilize ATF4 protein. By electrophoretic mobility shift assay (EMSA) using purified GST-Hop2 and His-ATF4 and radiolabeled OSE1 as a probe, we found that His-ATF4/OSE1 complex was not affected by the addition of increased amount of GST-Hop2 or GST control (Fig. 7F). This result revealed that Hop2 does not affect ATF4 to bind OSE1 DNA. In addition, GST alone failed to bind OSE1 in EMSA (data not shown), which is consistent with the fact that Hop2 lacks basic domain. To test the second possibility, we performed Western blot analysis of the nuclear extracts from MC3T3-E1 osteoblast precursor cells stably overexpressing Hop2. Fig. 7G, H showed that Hop2 overexpression tripled the total amount of nuclear ATF4 protein without affecting its mRNA level. More importantly, the

endogenous ATF4 level in *Hop2*$^{-/-}$ primary calvaria was lower than that in WT calvaria (Fig. 7I), suggesting that the interaction of Hop2 and ATF4 stabilizes the latter in these cells. This explains, at least in part, our previous observation that ATF4 was only detected in osteoblasts but not in non-osteoblastic cells.[3] Taken together, these results indicate that Hop2 enhances ATF4-mediated transcription and osteoblast differentiation in vitro by increasing the pool of endogenous ATF4 protein. Based on the findings presented herein, we propose that Hop2 modulates the activity of ATF4 by stabilizing its protein in committed osteoblasts to promote osteoblast differentiation and function (Fig. 8).

Discussion

In this study, we have provided molecular and genetic data establishing Hop2 as a transcriptional partner of ATF4. Hop2 was originally discovered in yeast by genetic screening[25,30] and later studies in both yeast and mammals showed that it acts as a meiotic-specific protein to facilitate proper alignment/pairing between homologous chromosomes.[31] Mice lacking *Hop2* (*Hop2*$^{-/-}$) are infertile with absence of gametogenesis due to a mitotic arrest at prophase,[23] whereas human *HOP2* mutations are found in patients with breast and ovarian cancer, as well as in patients with gonadal dysgenesis.[32,33] This study is the first demonstration that Hop2 plays a biological role in extra-reproductive organs. By directly binding to ATF4 via its Zip domain, Hop2 enhanced ATF4-mediated transcription of target genes, accelerated osteoblast differentiation, and increased the protein content of ATF4. Moreover, similar to *Atf4*$^{-/-}$ mice, the *Hop2*$^{-/-}$ mice as well as the *Atf4*$^{+/-}$:*Hop2*$^{+/-}$ compound heterozygous mutant mice display low bone mass phenotype. Compared with those of WT or single heterozygous controls,[9] the primary MSCs from the bone marrow of *Hop2*$^{-/-}$ and *Atf4*$^{+/-}$:*Hop2*$^{+/-}$ mice display 1) reduced expression of the osteoblast differentiation marker *Ocn* and 2) defective synthesis of type I collagen, two major characteristics identical to the ones of *Atf4*$^{-/-}$ osteoblasts. Although we were able to co-localize ATF4 and Hop2 in calvaria osteoblast cultures, we did not succeed in showing co-localization in osteoblasts in vivo on bone tissue sections. This caveat can stem from several factors, including the low level of expression of these proteins in bone, similarly to other important transcription factors such as Gli or Runx2, and/or from the unavailability of good antibodies against ATF4 and Hop2 and/or the fact that ATF4 is a protein involved in stress response, hence its higher expression in osteoblast cultures versus in vivo. Based on these lines of molecular and genetic evidence, we conclude that Hop2 is a physiological coactivator of a bona fide osteoblast transcription factor.

Milder skeletal defects in *Hop2*$^{-/-}$ mice than the ones found in *Atf4*$^{-/-}$ mice suggest that the *Hop2* deficiency phenotypes arise primarily from a failure of osteoblasts to execute ATF4 functions. This is expected because, first, Hop2 has no selectivity in DNA binding, which is consistent with the fact that it does not contain a basic region, a motif responsible for specific DNA recognition, and, second, the conserved basic residues of ATF4 basic domain orient in a position favoring specific DNA binding when it forms heterodimers with other bZip partners.[34] Interestingly, we have observed an increased fat mass in the *Hop2*$^{-/-}$ mice (data not shown), which is the opposite to what has been reported to the lean phenotype of the *Atf4*$^{-/-}$ mice.[12,13] The molecular mechanisms by which Hop2 contributes to fat formation is unclear and under our investigation at the moment. The absence of

developmental abnormalities in *Hop2*$^{-/-}$ mice, including absence of short stature, suggests that Hop2 is not required for the reported chondrocytic functions of ATF4.[21,29] It remains to be seen what biological role that Hop2 plays during early embryonic development, given its expressed has been observed in E11 to E17 mouse embryos[26] and our finding that ATF4 also directly regulates the transcription of *Indian hedgehog*.[29] Furthermore, we have observed a progressive increase in the mRNA of *RankL* in cultured *Hop2*$^{-/-}$ BMSCs along with the differentiation stages (Supplemental Fig. S2C). However, we did not detect increased number of osteoclasts on the bone surface of the *Hop2*$^{-/-}$ bones, suggesting that the effect of Hop2 on ATF4 is more important at the early stage of osteoblast differentiation. This is also supported by our Western blot analysis (Fig. 7I) and the data reported by other groups showing that hypertrophic chondrocytes and osteocytes are the main sources of physiological RankL that is responsible for the osteoclastogenesis.[35,36] The global nature of the *Hop2*$^{-/-}$ and *Atf4*$^{+/-}$: *Hop2*$^{+/-}$ mice does not firmly exclude possible additional mechanisms explaining the low bone mass phenotype. It also remains to be seen whether the serum level of uncarboxylated Ocn is affected in *Hop2*$^{-/-}$ and *Atf4*$^{+/-}$:*Hop2*$^{+/-}$ mice. This is relevant because the Ocn is one of the major transcriptional target genes of ATF4 osteoblasts and its uncarboxylated Ocn is the active form of this bone-derived hormone responsible for its regulation of glucose and energy metabolism.[37] The osteopenic phenotype found raises the possibility that Hop2 in vivo may fine-tune the activity of ATF4 in osteoblasts to determine the amount of bone formation by possibly dialing the level of Ocn.

As a bZip member, the mRNA of ATF4 is ubiquitously expressed, but its protein level is undetectable in many cell types and tissues except for chondrocytes and osteoblasts.[2–4,9,29] It is currently unknown whether overexpression of Hop2 and enhanced ATF4 protein level is due to its ability to prevent the latter from proteasome degradation, a known mechanism likely determining the location and time at which ATF4 protein is expressed.[3] Because purified Hop2 did not interfere ATF4 to bind its cognate DNA and the Zip domain containing truncated Hop2$^{81-147}$ is sufficient to augment the activity of ATF4, we speculate that the dimerization of Hop2 and ATF4 may prevent the latter to be undergoing the proteasomal degradation pathway. Interestingly, as homodimers of ATF4 have been shown to be thermodynamically unstable,[34,38] the heterodimer partners of ATF4 influencing its stability in specific cell types, such as osteoblasts, could be an important mechanism by which the specific distribution and activity of ATF4 are controlled. Furthermore, since phosphorylation of ATF4S219 and acetylation of ATF4K311 are both critical for its stability,[39,40] it would be of interest to test whether Hop2 affects such post-translational modifications.

Different from other bZip eukaryotic transcription factors, Hop2 lacks the basic region in front of the Zip motif. This structural feature is consistent with the observation that Hop2 binds both double-stranded and single-stranded DNA with no sequence specificity,[23,25] which also explains why no transcriptional targets of Hop2 have been reported so far. Another structural feature is that the Zip motif is only present in the mammalian Hop2, not in its yeast ortholog. Although the origin of this Zip motif is currently unclear, it provides the structural basis for its divergent functions by dimerizing with other bZip transcription factors with DNA binding specificity. The third structural feature of Hop2 is that it has a highly conserved acidic domain at the end of C-terminus.[41] Whether this domain

contributes to the enhanced transcriptional activity of ATF4 remains to be tested in the near future.

In conclusion, for the first time to our knowledge, our data identify that Hop2 is a physiological partner of ATF4 in osteoblasts, which supports a somatic function of this DNA recombinase in addition to its well-known activity to regulate homologous chromosomal pairing. Mechanistically, we found the Zip domain of Hop2 is responsible for its binding to ATF4 and its stabilization in osteoblasts. However, it remains unknown whether Hop2 stabilizes ATF4 by blocking its ubiquitination, which may subsequently prevent ATF4 from proteosomal degradation.[3] It will also be of interest to test whether steroid hormones, thyroid hormones, retinoic acid, and vitamin D3 act upstream of Hop2 in osteoblasts or MSCs. These steroids are known to play important roles in the regulation of bone metabolism and more relevantly have been shown to bind to nuclear receptors that were previously shown to interact with Hop2 in vitro.[26] Therefore, we expect our novel identification of Hop2 as ATF4 in mature osteoblasts will pave the way to further our understanding of ATF4 biology in adults.

Supplementary Material

Refer to Web version on PubMed Central for supplementary material.

Acknowledgments

We thank Dr Florent Elefteriou, Gerard Karsenty, and Brendan Lee for helpful suggestions; the Rolanette and Berdon Lawrence Bone Disease Program of Texas and Baylor College of Medicine (BCM) Center for Skeletal Medicine and Biology for assistance in skeletal phenotypic analysis; and Yue Hu and Louis R Bourgogne for proofreading. This work was supported by the NIH (grant R01AR067303 to XY).

References

1. Nakashima K, Zhou X, Kunkel G, et al. The novel zinc finger-containing transcription factor osterix is required for osteoblast differentiation and bone formation. Cell. 2002;108(1):17–29. [PubMed: 11792318]
2. Ducy P, Karsenty G. Two distinct osteoblast-specific cis-acting elements control expression of a mouse osteocalcin gene. Mol Cell Biol. 1995;15(4):1858–69. [PubMed: 7891679]
3. Yang X, Karsenty G. ATF4, the osteoblast accumulation of which is determined post-translationally, can induce osteoblast-specific gene expression in non-osteoblastic cells. J Biol Chem. 2004;279(45):47109–14. [PubMed: 15377660]
4. Schinke T, Karsenty G. Characterization of Osf1, an osteoblast-specific transcription factor binding to a critical cis-acting element in the mouse osteocalcin promoters. J Biol Chem. 1999;274(42):30182–9. [PubMed: 10514508]
5. Sheu Y, Cauley JA. The role of bone marrow and visceral fat on bone metabolism. Curr Osteoporos Rep. 2011;9(2):67–75. [PubMed: 21374105]
6. Vinson CR, Conover S, Adler PN. A Drosophila tissue polarity locus encodes a protein containing seven potential transmembrane domains. Nature. 1989;338(6212):263. [PubMed: 2493583]
7. Williams SC, Cantwell CA, Johnson PF. A family of C/EBP-related proteins capable of forming covalently linked leucine zipper dimers in vitro. Genes Dev. 1991;5(9):1553–67. [PubMed: 1884998]
8. Xiao G, Jiang D, Ge C, et al. Cooperative interactions between activating transcription factor 4 and Runx2/Cbfa1 stimulate osteoblast-specific osteocalcin gene expression. J Biol Chem. 2005;280(35):30689–96. [PubMed: 16000305]

9. Yang X, Matsuda K, Bialek P, et al. ATF4 is a substrate of RSK2 and an essential regulator of osteoblast biology: implication for Coffin-Lowry syndrome. Cell. 2004;117(3):387–98. [PubMed: 15109498]
10. Tanaka T, Tsujimura T, Takeda K, et al. Targeted disruption of ATF4 discloses its essential role in the formation of eye lens fibres. Genes Cells. 1998;3(12):801–10. [PubMed: 10096021]
11. Hettmann T, Barton K, Leiden JM. Microphthalmia due to p53-mediated apoptosis of anterior lens epithelial cells in mice lacking the CREB-2 transcription factor. Dev Biol. 2000;222(1):110–23. [PubMed: 10885750]
12. Masuoka HC, Townes TM. Targeted disruption of the activating transcription factor 4 gene results in severe fetal anemia in mice. Blood. 2002;99(3):736–45. [PubMed: 11806972]
13. Yoshizawa T, Hinoi E, Jung DY, et al. The transcription factor ATF4 regulates glucose metabolism in mice through its expression in osteoblasts. J Clin Invest. 2009;119(9):2807–17. [PubMed: 19726872]
14. Harding HP, Novoa I, Zhang Y, et al. Regulated translation initiation controls stress-induced gene expression in mammalian cells. Mol Cell. 2000;6(5):1099–108. [PubMed: 11106749]
15. Harding HP, Zhang Y, Bertolotti A, Zeng H, Ron D. Perk is essential for translational regulation and cell survival during the unfolded protein response. Mol Cell. 2000;5(5):897–904. [PubMed: 10882126]
16. Lian N, Wang W, Li L, Elefteriou F, Yang X. Vimentin inhibits ATF4-mediated osteocalcin transcription and osteoblast differentiation. J Biol Chem. 2009;284(44):30518–25. [PubMed: 19726676]
17. Lian N, Lin T, Liu W, et al. Transforming growth factor β suppresses osteoblast differentiation via the vimentin activating transcription factor 4 (ATF4) axis. J Biol Chem. 2012;287(43):35975–84. [PubMed: 22952236]
18. Kilkenny C, Browne WJ, Cuthill IC, Emerson M, Altman DG. Improving bioscience research reporting: the ARRIVE guidelines for reporting animal research. PLoS Biol. 2010;8(6):e1000412. [PubMed: 20613859]
19. Yang X, Ji X, Shi X, Cao X. Smad1 domains interacting with Hoxc−8 induce osteoblast differentiation. J Biol Chem. 2000;275(2):1065–72. [PubMed: 10625647]
20. Virtanen P, Isotupa K. Staining properties of alizarin red S for growing bone in vitro. Cells Tissues Organs. 1980;108(2):202–7.
21. Wang W, Lian N, Ma Y, et al. Chondrocytic Atf4 regulates osteoblast differentiation and function via Ihh. Development. 2012;139(3):601–11. [PubMed: 22190639]
22. Dempster DW, Compston JE, Drezner MK, et al. Standardized nomenclature, symbols, and units for bone histomorphometry: a 2012 update of the report of the ASBMR Histomorphometry Nomenclature Committee. J Bone Miner Res. 2013;28(1):2–17. [PubMed: 23197339]
23. Petukhova GV, Romanienko PJ, Camerini-Otero RD. The Hop2 protein has a direct role in promoting interhomolog interactions during mouse meiosis. Dev Cell. 2003;5(6):927–36. [PubMed: 14667414]
24. Peng M, Bakker JL, DiCioccio RA, et al. Inactivating mutations in GT198 in familial and early-onset breast and ovarian cancers. Genes Cancer. 2013;4(1–2):15–25. [PubMed: 23946868]
25. Pezza RJ, Voloshin ON, Volodin AA, et al. The dual role of HOP2 in mammalian meiotic homologous recombination. Nucleic Acids Res. 2013;42(4):2346–57. [PubMed: 24304900]
26. Ko L, Cardona GR, Henrion-Caude A, Chin WW. Identification and characterization of a tissue-specific coactivator, GT198, that interacts with the DNA-binding domains of nuclear receptors. Mol Cell Biol. 2002;22(1):357–69. [PubMed: 11739747]
27. Wang S-Z, Ou J, Zhu LJ, Green MR. Transcription factor ATF5 is required for terminal differentiation and survival of olfactory sensory neurons. Proc Natl Acad Sci U S A. 2012;109 (45):18589–94. [PubMed: 23090999]
28. Kanazawa I, Yamaguchi T, Yamamoto M, et al. Serum osteocalcin level is associated with glucose metabolism and atherosclerosis parameters in type 2 diabetes mellitus. J Clin Endocrinol Metabol. 2009;94(1):45–9.

29. Wang W, Lian N, Li L, et al. Atf4 regulates chondrocyte proliferation and differentiation during endochondral ossification by activating Ihh transcription. Development. 2009;136(24):4143–53. [PubMed: 19906842]
30. Leu J-Y, Chua PR, Roeder GS. The meiosis-specific Hop2 protein of *S. cerevisiae* ensures synapsis between homologous chromosomes. Cell. 1998;94(3):375–86. [PubMed: 9708739]
31. Tsubouchi H, Roeder GS. The importance of genetic recombination for fidelity of chromosome pairing in meiosis. Dev Cell. 2003;5(6): 915–25. [PubMed: 14667413]
32. Lefterova MI, Haakonsson AK, Lazar MA, Mandrup S. PPARγ and the global map of adipogenesis and beyond. Trends Endocrinol Metab. 2014;25(6):293–302. [PubMed: 24793638]
33. Wilson DR, Juan T, Wilde M, Fey G, Darlington G. A 58-base-pair region of the human C3 gene confers synergistic inducibility by interleukin−1 and interleukin−6. Mol Cell Biol. 1990;10(12):6181–91. [PubMed: 2247055]
34. Podust LM, Krezel AM, Kim Y. Crystal structure of the CCAAT box/enhancer-binding protein β activating transcription factor−4 basic leucine zipper heterodimer in the absence of DNA. J Biol Chem. 2001; 276(1):505–13. [PubMed: 11018027]
35. Nakashima T, Hayashi M, Fukunaga T, et al. Evidence for osteocyte regulation of bone homeostasis through RANKL expression. Nat Med. 2011;17(10):1231. [PubMed: 21909105]
36. Xiong J, Onal M, Jilka RL, Weinstein RS, Manolagas SC, O'Brien CA. Matrix-embedded cells control osteoclast formation. Nat Med. 2011;17(10):1235. [PubMed: 21909103]
37. Rached M-T, Kode A, Silva BC, et al. FoxO1 expression in osteoblasts regulates glucose homeostasis through regulation of osteocalcin in mice. J Clin Invest. 2010;120(1):357–68. [PubMed: 20038793]
38. Vinson C, Hai T, Boyd S. Dimerization specificity of the leucine zipper-containing bZIP motif on DNA binding: prediction and rational design. Genes Dev. 1993;7(6):1047–58. [PubMed: 8504929]
39. Lassot I, Ségéral E, Berlioz-Torrent C, et al. ATF4 degradation relies on a phosphorylation-dependent interaction with the SCFβTrCPUbiquitin ligase. Mol Cell Biol. 2001;21(6): 2192–202. [PubMed: 11238952]
40. Lassot I, Estrabaud E, Emiliani S, et al. p300 modulates ATF4 stability and transcriptional activity independently of its acetyltransferase domain. J Biol Chem. 2005;280(50):41537–45. [PubMed: 16219772]
41. Juan T, Wilson DR, Wilde MD, Darlington GJ. Participation of the transcription factor C/EBP delta in the acute-phase regulation of the human gene for complement component C3. Proc Natl Acad Sci U S A. 1993;90(7):2584–8. [PubMed: 8385337]

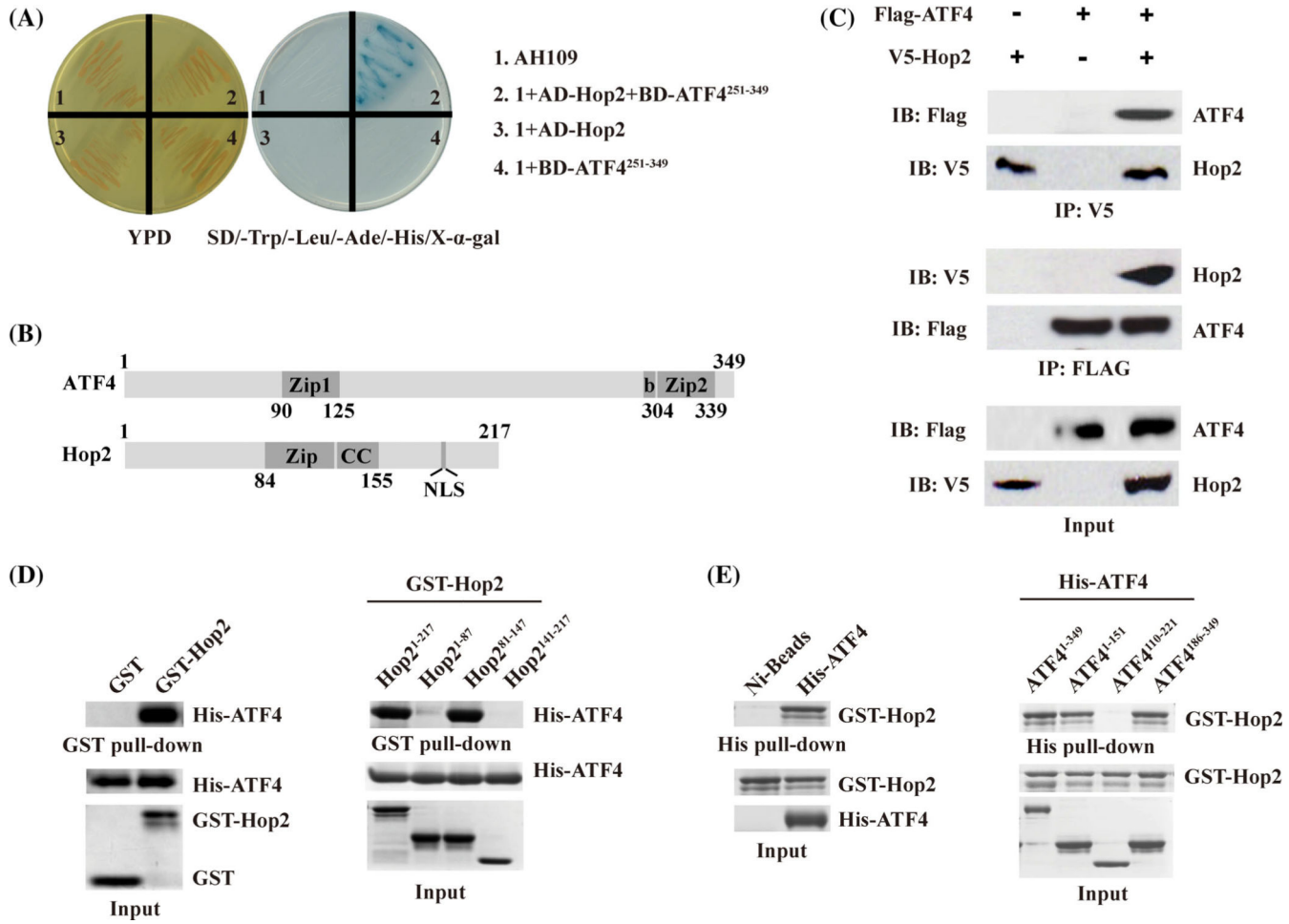

Fig. 1.

Identification of Hop2 as an ATF4-interacting protein. (*A*) Identification of Hop2 in yeast two-hybrid assay. YPD = yeast extract, peptone, and dextrose growth medium; SD = synthetic defined base; AD = activation domain; BD = DNA binding domain. (*B*) Schematic illustration of Hop2 and ATF4 primary structures. LZ = leucine zipper domain; b = basic amino acid-rich domain; CC = coiled-coil structure; NLS = nuclear localization signal. (*C*) Co-immunoprecipitation of Hop2 and ATF4 in nuclear extractions (NEs) of COS1 cells ectopically expressing V5-tagged Hop2 and Flag-tagged ATF4. (*D*) Pulldown assay showing that GST-Hop2 binds directly to His-ATF4 purified from bacteria (left panel). The leucine zipper (LZ) domain of Hop2 is sufficient to bind His-ATF4 (right panel). (*E*) Pulldown assay using His-ATF4 and Ni-NTA resin column showing that His-ATF4 binds directly to GST-Hop2 (left panel). The LZ domains of ATF4 interact directly with GST-Hop2 (right panel).

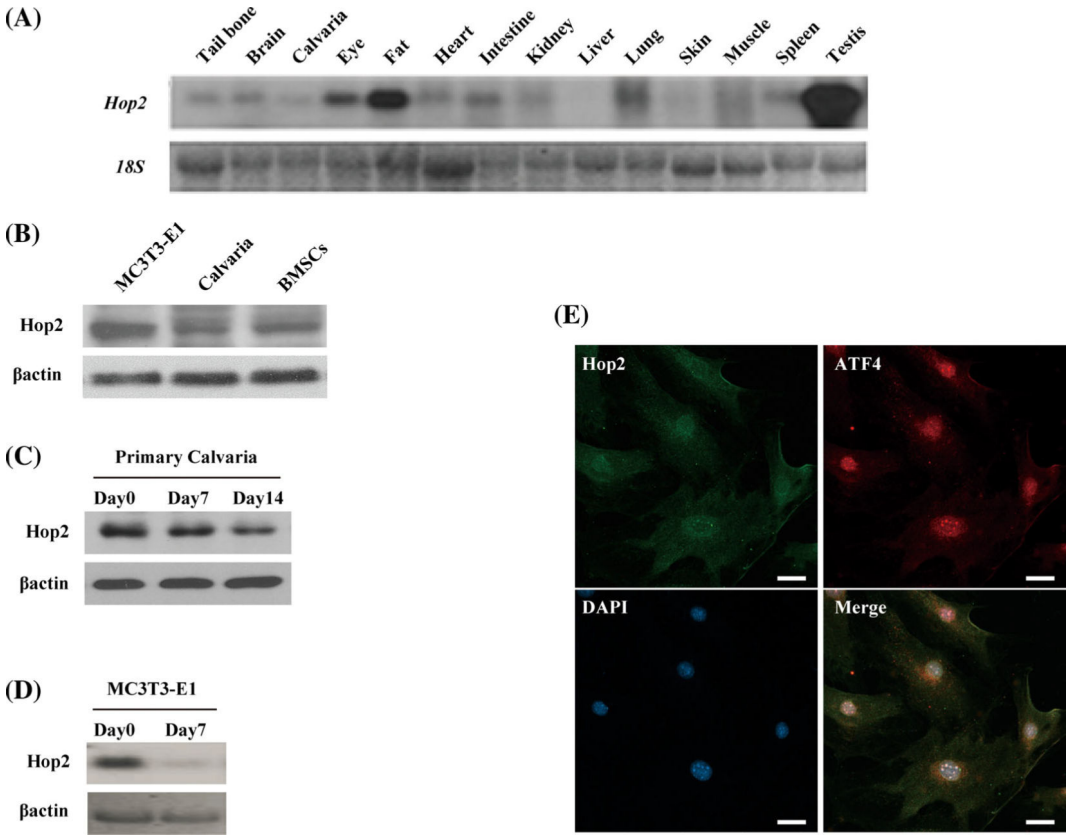

Fig. 2.

Hop2 is expressed in osteoblasts. (*A*) Northern blot analysis showing the expression pattern of *Hop2*. *18S*, loading control. (*B*) Western blot analysis of Hop2 expression in nuclear extractions (NEs) from MC3T3-E1 cells, primary calvaria, and bone marrow stromal cells (BMSCs). (*C*) Western blot analysis of Hop2 expression in primary calvaria during osteoblastic differentiation in vitro. (*D*) Western blot analysis of Hop2 expression in MC3T3-E1 cells during osteogenic differentiation. Note that Hop2 expresses at higher level in preosteoblasts than differentiated osteoblasts. (*E*) Immunofluorescence staining showing co-localization of Hop2 (green) and ATF4 (red) in primary calvaria cells. Scale bars = 20 μm.

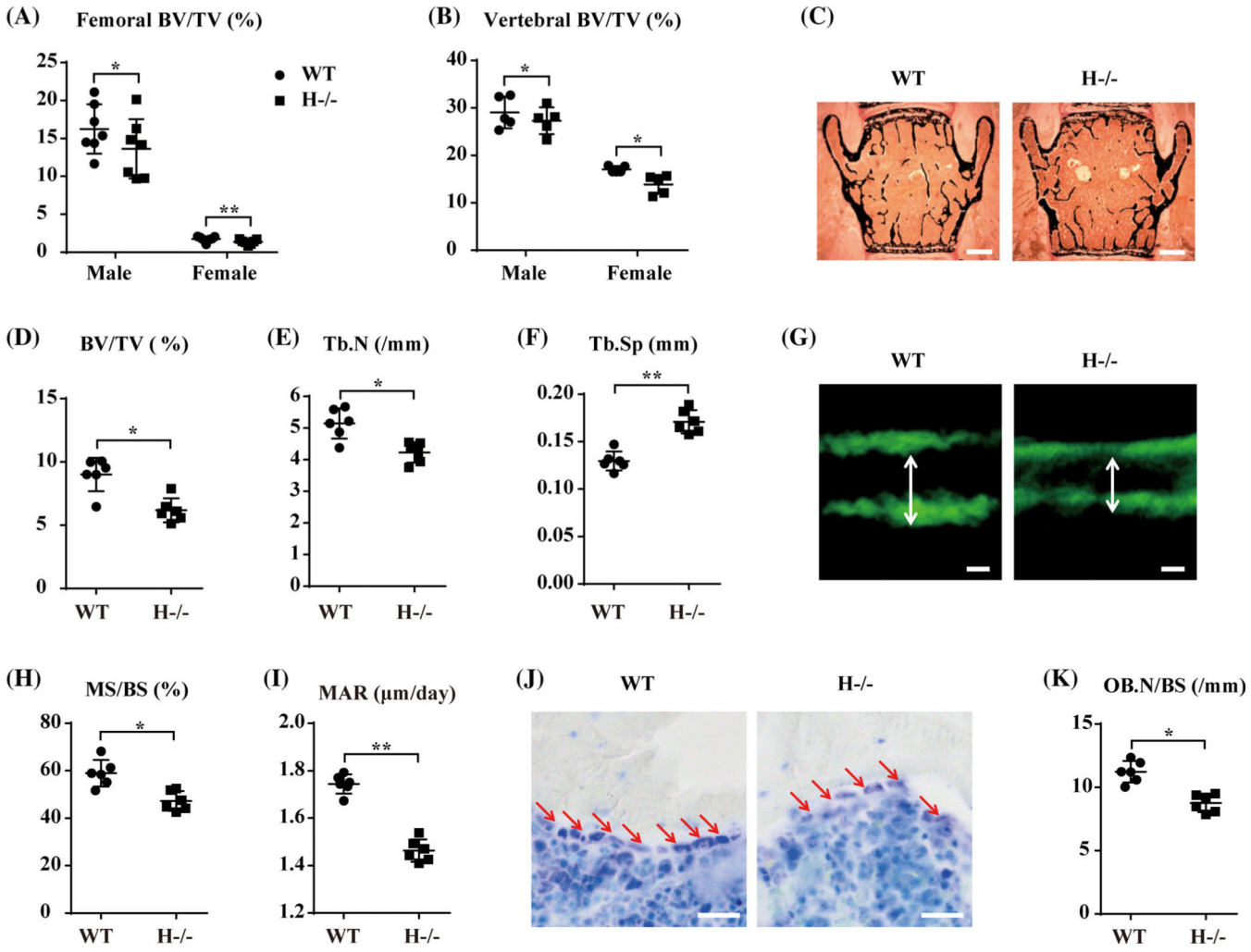

Fig. 3.

Hop2−/− mice display osteopenic phenotype. (*A*, *B*) Bone volume/tissue volume (BV/TV) of 6-month femur (*A*, $n = 7$) and vertebrae (*B*, $n = 5$), measured by μCT showing decreased bone mass in *Hop2*−/− mice (H−/−) compared with WT littermates (Ctrl) of indicated sexes. (*C*–*K*) Histology and histomorphometry analyses of female mice. Von Kossa-stained spine sections showing trabecular bone of *Hop2*−/− mice compared with wild type (WT) (*C*). Scale bars = 500 μm. Decreased BV/TV (*D*), decreased trabecular number (Tb.N) (*E*), and increased trabecular separation (Tb.Sp) (*F*) of vertebrae detected in *Hop2*−/− mice and WT ($n = 6$). Calcein double labeling showing the mineralization ability of osteoblasts on the trabecular bone of spines from *Hop2*−/− mice and WT (*G*). Scale bars = 5 μm. Mineralizing surface/bone surface (MS/BS) (*H*) and mineral apposition rate (MAR) (*I*) are decreased in *Hop2*−/− mice compared with WT ($n = 6$). Toluidine blue-stained spine sections (*J*) show osteoblasts on the trabecular bone surface (red arrows). Scale bars = 50 μm. Osteoblast number/bone surface (OB.N/BS) is decreased in *Hop2*−/− mice compared with Ctrl ($n = 6$) (*K*). Paired *t* test was performed for the statistical analyses. Error bars represent the SD. *$p < 0.05$; **$p < 0.01$.

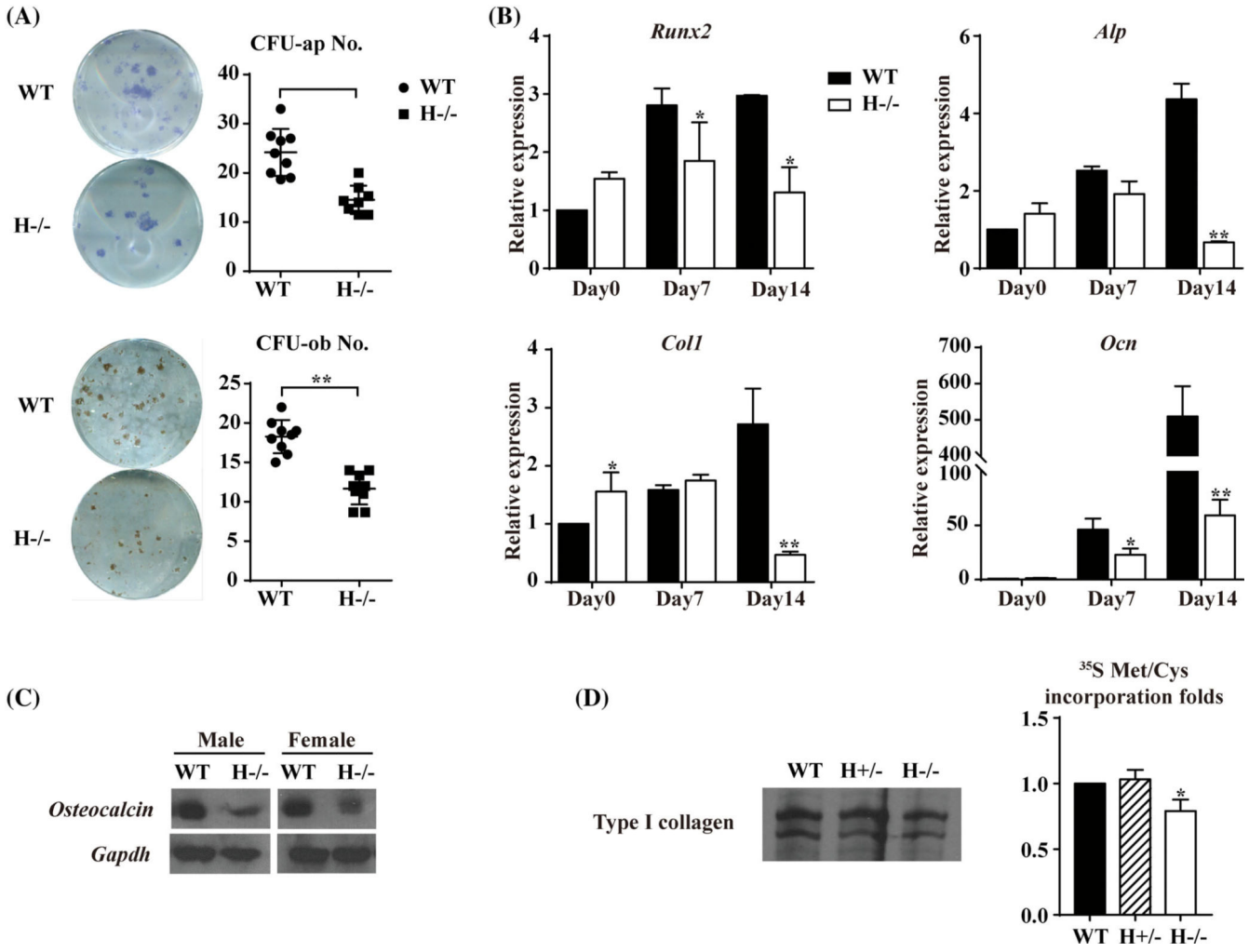

Fig. 4.

Hop2 regulates osteoblast differentiation and function cell autonomously. (*A*) Osteogenic differentiation assays of bone marrow stromal cells (BMSCs) isolated from *Hop2*−/− mice (H−/−) and their WT littermates ($n = 9$). CFU-ap = alkaline phosphatase–positive colony-forming units; CFU-ob = von Kossa-positive colony-forming units. (*B*) qRT-PCR of early osteoblast marker genes of *Runx2*, alkaline phosphatase (*Alp*), *type I collagen* α *chain* (*Col1*), and late gene of *Osteocalcin* (*Ocn*), showing impaired osteoblast differentiation in *Hop2*−/− BMSCs compared with Ctrl. (*C*) Northern blot analysis of *Osteocalcin* mRNA level in femur of *Hop2*−/− mice and WT. (*D*) Type I collagen synthesis analysis by 35S Met/Cys incorporation assay. Notice that both α1 and α2 chains of type I collagen are decreased in *Hop2*−/− osteoblasts compared with WT and single heterozygous control. *t* test was performed for the statistical analyses. Experiments were repeated three times. Error bars represent the SD. *$p < 0.05$; **$p < 0.01$.

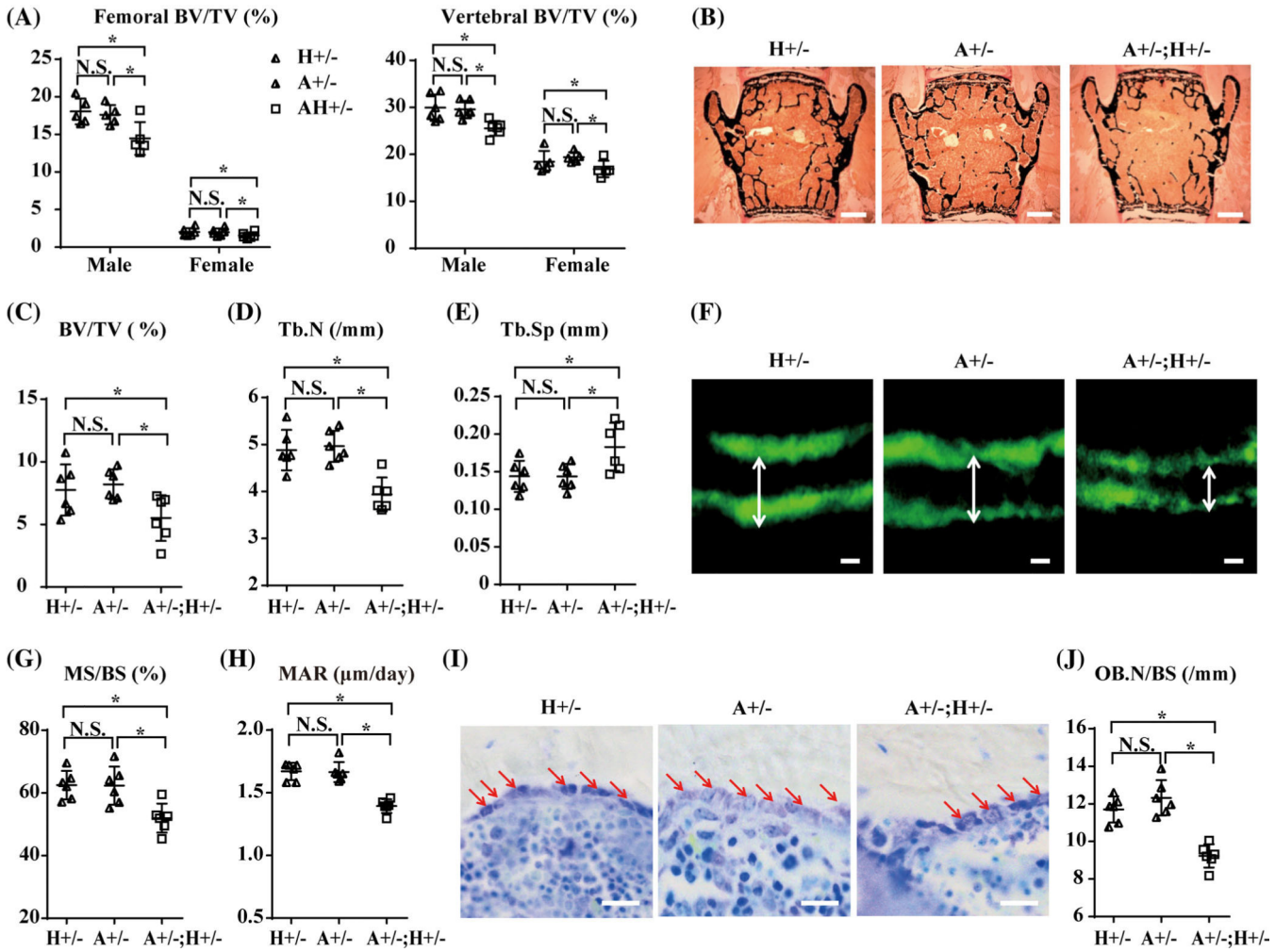

Fig. 5.

Genetic interaction between *Hop2* and *Atf4*. (*A*) Bone volume/tissue volume (BV/TV) of 6-month femur (left panel, $n = 5$) and vertebrae (right panel, $n = 6$) measured by μCT showing decreased bone mass in $Atf4^{+/-};Hop2^{+/-}$ mice ($A^{+/-};H^{+/-}$) compared with $Hop2^{+/-}$ ($H^{+/-}$) and $Atf4^{+/-}$ ($A^{+/-}$) littermates, of indicated sexes. (*B–J*) Histology and histomorphometry analyses of female mice. Von Kossa-stained spine sections showing trabecular bone of $Atf4^{+/-}$; $Hop2^{+/-}$ mice compared with $Hop2^{+/-}$ and $Atf4^{+/-}$ mice (*B*). Scale bars = 500 μm. Decreased BV/TV (*C*), decreased trabecular number (Tb.N) (*D*), and increased trabecular separation (Tb.Sp) (*E*) of vertebrae detected in $Atf4^{+/-};Hop2^{+/-}$ mice ($n = 6$). Calcein double labeling showing the mineralization ability of osteoblasts on the trabecular bone of spines from $Atf4^{+/-};Hop2^{+/-}$, $Hop2^{+/-}$ and $Atf4^{+/-}$ mice (*F*). Scale bars = 5 μm. Mineralizing surface/bone surface (MS/BS) (*G*) and mineral apposition rate (MAR) (*H*) are decreased in $Atf4^{+/-};Hop2^{+/-}$ mice compared with $Hop2^{+/-}$ and $Atf4^{+/-}$ mice ($n = 6$). Toluidine blue-stained spine sections (*I*) show osteoblasts on the trabecular bone surface (red arrows). Scale bars = 50 μm. Osteoblast number/bone surface (OB.N/BS) is decreased in $Atf4^{+/-};Hop2^{+/-}$ mice compared with $Hop2^{+/-}$ and $Atf4^{+/-}$ mice ($n = 6$) (*J*).

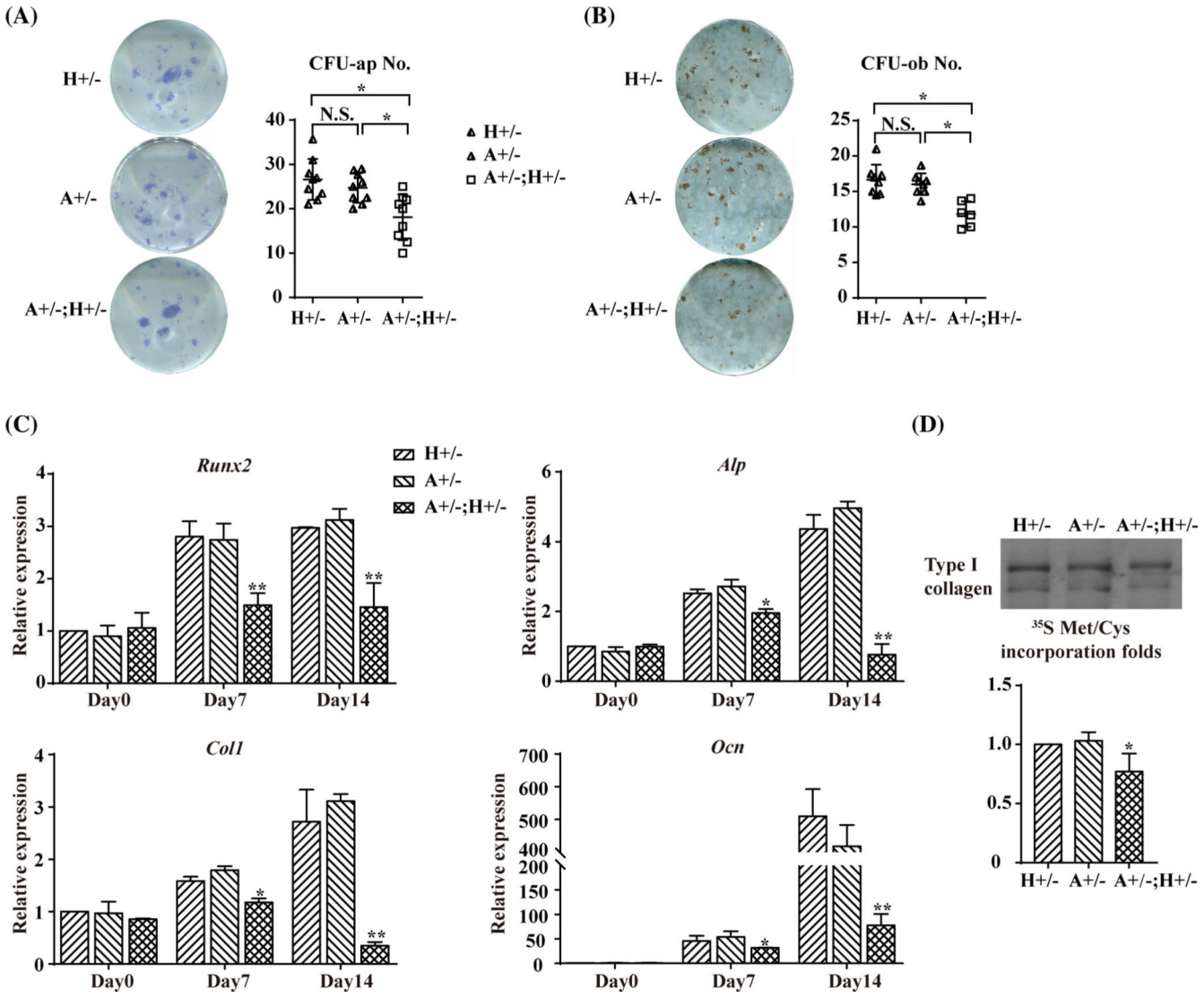

Fig. 6.

Impaired osteoblast differentiation of *Atf4*$^{+/-}$;*Hop2*$^{+/-}$ primary BMSCs. (*A*, *B*) Osteogenic differentiation assays of bone marrow stromal cells (BMSCs) isolated from *Atf4*$^{+/-}$;*Hop2*$^{+/-}$ mice, *Hop2*$^{+/-}$ and *Atf4*$^{+/-}$ mice. (*A*) CFU-ap = alkaline phosphatase–positive colony-forming units ($n = 9$). (*B*) CFU-ob = von Kossa-positive colony-forming units ($n = 8$). (*C*) qRT-PCR of early osteoblast marker genes of *Runx2*, alkaline phosphatase (*Alp*), *type I collagen* α *chain* (*Col1*), and late gene of *Osteocalcin* (*Ocn*), showing impaired osteoblast differentiation in *Atf4*$^{+/-}$;*Hop2*$^{+/-}$ BMSCs compared with *Hop2*$^{+/-}$ and *Atf*$^{+/-}$. (*D*) Type I collagen synthesis analysis by ^{35}S Met/Cys incorporation assay. Notice that both α1 and α2 chains of type I collagen are decreased in *Atf4*$^{+/-}$;*Hop2*$^{+/-}$ osteoblasts. *t* test was performed for the statistical analyses. Error bars represent the SD. *$p < 0.05$; **$p < 0.01$.

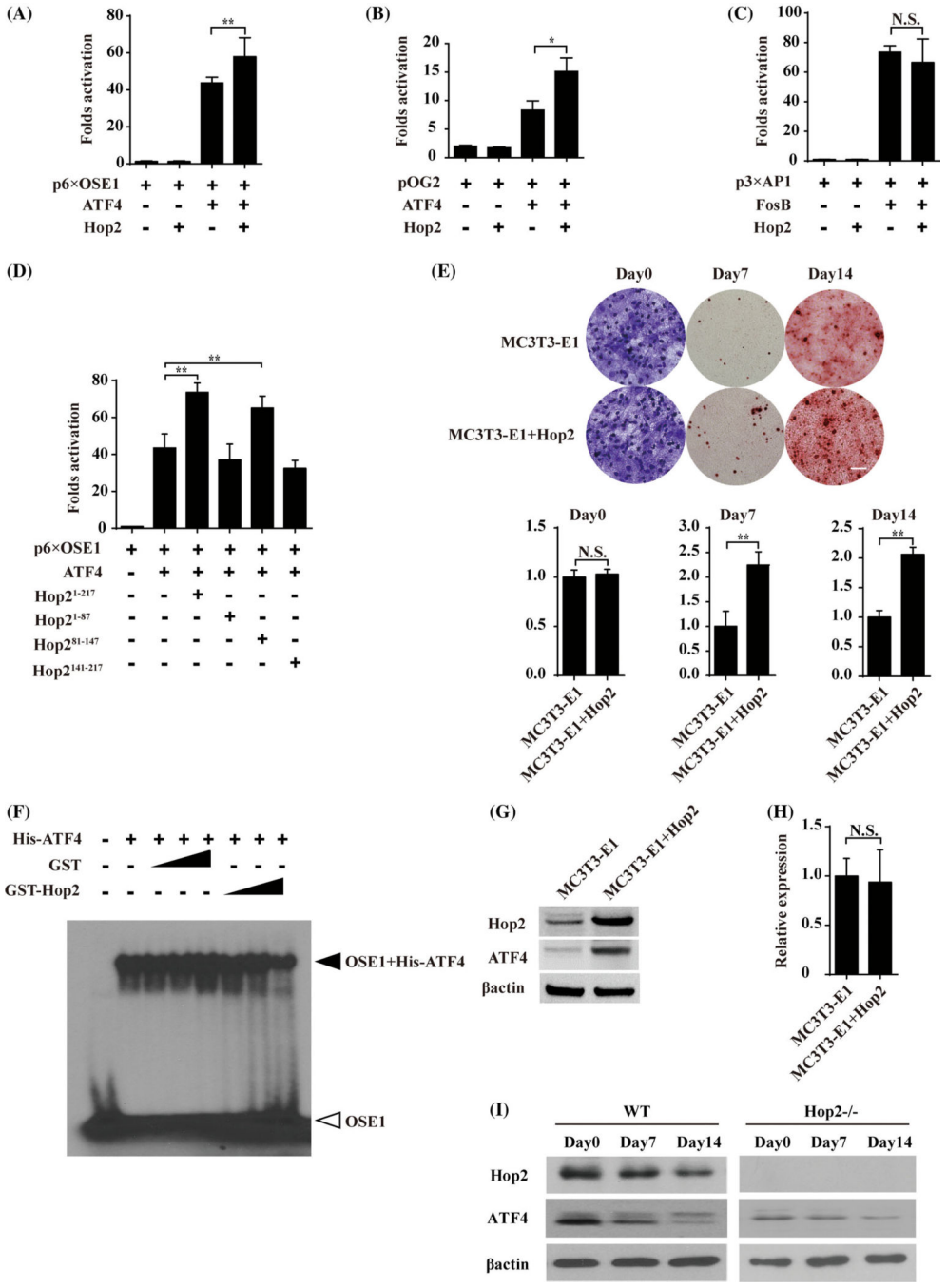

Fig. 7.

Hop2 enhances ATF4-mediated transcription and osteoblast differentiation. (*A–C*) DNA cotransfections of COS1 cells with indicated reporter constructs and/or the expression vectors of ATF4, Hop2, and FosB. (*D*) DNA cotransfections of COS1 cells with a reporter construct, p6×OSE1-luc, and the expression vectors of ATF4, full-length Hop2, and its truncated variants. (*E*) Osteogenic differentiation assay. Overexpression of Hop2 in MC3T3-E1 cells increased the number of Alizarin red S–stained cells. Equal number of cells plated on day 0 was shown by crystal violet staining. Notice that Hop2 overexpression increased

the number of Alizarin red S–stained cells on day 7 and day 14. Right panel shows the quantification of stains released from cultures of indicated days. Scale bars = 250 μm. (*F*) EMSA showing purified GST-Hop2 has no effect on purified His-ATF4 binding to its cognate DNA probe. (*G*) Western blot analysis of nuclear extractions (NEs) from MC3T3-E1 cells overexpressing Hop2. Notice that the endogenous ATF4 is increased. (*H*) qRT-PCR of *Atf4* mRNA level showing there is no difference in MC3T3-E1 cells and those overexpressing Hop2. (*I*) Western blot analysis of NEs from primary calvaria cells showing that ATF4 decreases to a lower extent in $Hop2^{-/-}$ cells, during induced osteoblast differentiation. *t* test was performed for the statistical analyses. Error bars represent the SD. $*p < 0.05$; $**p < 0.01$.

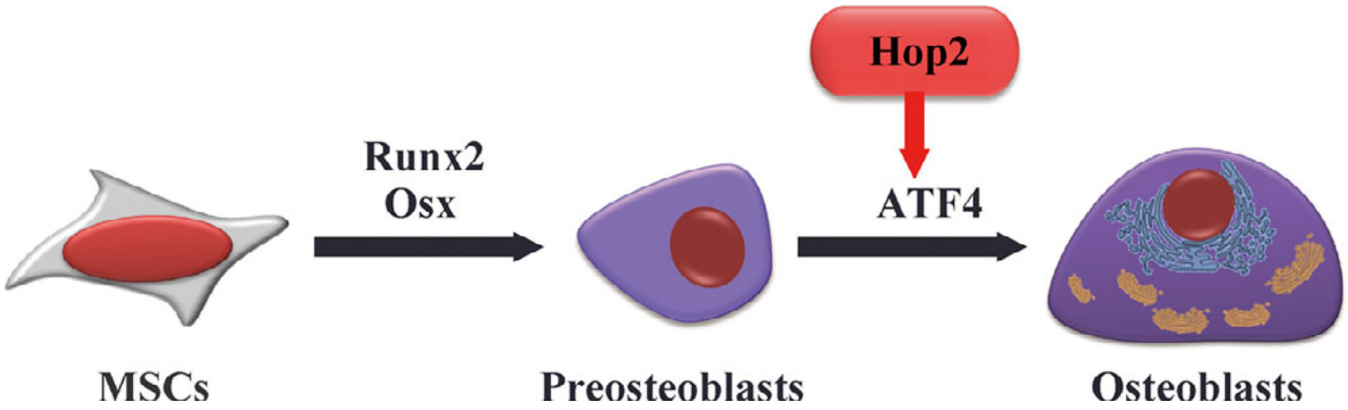

Fig. 8.

Working model of Hop2 during osteoblast differentiation. Hop2 modulates the activity of ATF4 in pre-osteoblasts. The dimerization of Hop2 and ATF4 promotes MSCs to become osteoblasts.

Table 1.

Born Ratio of *Hop2*$^{+/-}$ Mice

***Hop2* genotype**	**Wild type ($H^{+/+}$)**	**Heterozygotes ($H^{+/-}$)**	**Homozygotes ($H^{-/-}$)**
No.	68	102	49
Ratio (%)	31.05	46.58	22.37
Decreased bone mass	0	0	49